Food Bioscience 56 (2023) 103198

Contents lists available at ScienceDirect

Food Bioscience

journal homepage: www.elsevier.com/locate/fbio

Investigating the effectiveness of coacervates produced from conjugated and unconjugated *Spirulina* protein in delivering unstable oil to the intestinal phase of digestion

Zijia Zhang [a,*], Bo Wang [b], Greg Holden [c], Jie Chen [d], Benu Adhikari [a,e,**]

[a] School of Science, RMIT University, Melbourne, VIC 3083, Australia
[b] School of Behavioural and Health Science, Australian Catholic University, Sydney, NSW 2060, Australia
[c] Bega Corporate Centre, Melbourne, VIC 3008, Australia
[d] State Key Laboratory of Food Science and Resources, Jiangnan University, Wuxi, China
[e] Centre for Advanced Materials and Industrial Chemistry (CAMIC), RMIT University, Melbourne, VIC 3001, Australia

ARTICLE INFO

Keywords:
Spirulina protein concentrate
Conjugation
Complex coacervation
Microencapsulation
In-vitro digestion

ABSTRACT

This study investigated the potential of complex coacervates produced using *Spirulina* protein concentrate (SPC) conjugated with maltodextrin (MD) and carrageenan (CG) for encapsulating and delivering sensitive oils. A wet-heating Maillard reaction was employed to conjugate SPC with MD, followed by coacervation with CG to form the conjugate-based coacervates. Additionally, a mixture of unconjugated SPC and MD was coacervated with CG to produce mixture-based coacervates. Both types of coacervates were utilised as wall materials for encapsulating canola oil. The *in-vitro* digestion of the resulting microcapsules was assessed in oral, gastric, and intestinal phases, focusing on physicochemical parameters such as droplet size, zeta-potential, microstructure, proteolysis, oil release and lipolysis. The findings revealed that microcapsules prepared using both (SPC-MD mixture)-CG and (SPC-MD conjugate)-CG coacervates were remarkably stable against gastric digestion, as evidenced by the minimal production of free amino acids (15 mM). Most of the encapsulated oil (62–67%) was released during the intestinal phase due to the breakdown of the coacervates. Notably, the microcapsules produced with (SPC-MD conjugate)-CG coacervates demonstrated a lower degree of lipolysis (41.77% free fatty acid content) compared to those prepared with (SPC-MD mixture)-CG coacervates (53.35% free fatty acid content). These results highlight the potential of complex coacervates produced using conjugated SPC as promising materials for the encapsulation and delivery of sensitive oils.

1. Introduction

Nowadays, the foods we consume are expected not only to satisfy our basic hunger needs but also provide health benefits to our bodies. The later aspect is driving the development of functional foods, which are rich in bioactive compounds with proven health benefits. For example, oils that are rich in polyunsaturated fatty acids (PUFAs) are considered as functional ingredients. However, PUFAs are susceptible to adverse environmental and processing factors. Their oxidation and degradation often lead to the formation of toxic compounds and undesirable odour (Gogus & Smith, 2010). To overcome this problem, PUFAs are encapsulated, and the powder microcapsules are used as ingredients by the food industry. A typical microencapsulation process involves physically entrapping the oil in a single substance or combined multiple substances (known as wall material), thereby enhancing their physicochemical stability (Soleimanifar et al., 2020). Microencapsulation may also improve the stability of bioactive compounds during digestion to achieve controlled-release (Corrêa-Filho et al., 2019). However, the pattern of release, uptake, and bioavailability of the entrapped oil depends on the composition of the wall materials.

It is important to investigate the digestion (release and breakdown) of the stabilised oils from the microcapsules that utilise newly developed wall materials in order to ensure the efficacy and effectiveness of delivery (Dias et al., 2015). The *in-vitro* digestion method, particularly the one established through international consensus (INFOGEST), is commonly used for this purpose. This method simulates the

* Corresponding author.
** Corresponding author. School of Science, RMIT University, Melbourne, VIC 3083, Australia.
E-mail addresses: s3714749@student.rmit.edu.au (Z. Zhang), benu.adhikari@rmit.edu.au (B. Adhikari).

https://doi.org/10.1016/j.fbio.2023.103198
Received 11 June 2023; Received in revised form 18 August 2023; Accepted 25 September 2023
Available online 29 September 2023

gastrointestinal tract (GIT) environment using simulated digestive fluids and mimicking the physiological processes that occur during food digestion (Donhowe & Kong, 2014). During the *in-vitro* digestion, the microcapsule wall materials are expected to degrade to release the encapsulated oil, followed by its digestion by lipase (McClements et al., 2008).

Several factors have been reported to affect the digestibility of oils. This include (a) gastrointestinal tract conditions such as types of enzymes, pH levels, bile salts concentration, temperature, shear forces (Ann Augustin et al., 2014; Lin et al., 2018) and (b) physicochemical properties of digested matrix such as oil droplet size, composition, and structure of the wall material (Golding et al., 2011; Singh et al., 2009; Timilsena et al., 2017). For instance, Bannikova et al. (2018) used alginate as wall material to encapsulate fish oil. The results of *in-vitro* digestion showed the release rate of the encapsulated oil remained stable in the gastric phase but increased significantly in the intestinal phase, suggesting that the encapsulated oil was protected against gastric digestion and most of the oil was released in the small intestine. However, most of the encapsulation systems are developed at neutral pH, so keeping the microcapsule integrity in the acidic gastric environment is challenging. The released oil in gastric stage of human digestion can be oxidatively degraded before it is metabolised and absorbed (Kanner & Lapidot, 2001). Therefore, it is important to ensure the microcapsules containing unstable oils stay intact before they are introduced into the digestive system's intestinal stage.

The control release behaviour of encapsulated oil can be influenced by the interactions (e.g., electrostatic, and covalent) between wall materials (Huang et al., 2021). Complex coacervates, formed through the interaction of proteins and polysaccharides, find practical use as carriers to protect and deliver sensitive materials. For instance, Ardestani et al. (2022) optimised the coacervation between sodium caseinate and high methoxyl pectin, resulting in the formation of coacervates that exhibited significantly improved heat resistance and enhanced protection of bioactive compounds. Wang et al. (2017) showed that the complex coacervation of lactoferrin with sodium alginate improved the stability of the lactoferrin in gastric stage of digestion by as much as 30% when compared with the uncomplexed one. Moreover, in Qiu et al. (2022)'s study, the complex coacervates formed between mung bean protein isolate and apricot peel pectin was used to stabilise rose essential oil. This protein-polysaccharide wall material was stable in the gastric phase and released the oil in the intestinal phase. While various studies have highlighted the appropriateness of complex coacervates as encapsulation materials (Hasanvand et al., 2018; Hasanvand & Rafe, 2018, 2019), the protein-polysaccharide conjugates formed through the Maillard reaction can serve as better wall materials for oxidation-sensitive oils due to their superior protective effect. The encapsulating wall material produced using protein-polysaccharide conjugates are known to produce thicker and compact shell around oil droplets, resist acidic and enzymatic hydrolysis (Nooshkam & Varidi, 2020). These qualities make the conjugates excellent options for enhancing the stability of encapsulated oils during digestion (Nooshkam & Varidi, 2020). Yang et al. (2015) compared of the *in-vitro* digestion process of oil-in-water (O/W) emulsions stabilised by the physical mixture and conjugates of protein and soluble polysaccharide of soybean. The result showed that the conjugate-stabilised emulsion exhibited better stability than the one stabilised by the physical mixture in the simulated gastrointestinal conditions. However, to the best of our knowledge, there is still a lack of research on the digestibility of encapsulated oils stabilised by coacervates based on conjugates produced using Maillard reaction. The breakdown of such protein-polysaccharide conjugates and their complex coacervates in the digestion process is not adequately understood.

We reported Maillard reaction-based conjugation between *Spirulina* protein concentrate (SPC) and maltodextrin (MD) followed by their complex coacervation with carrageenan (CG) and used both conjugates and coacervates to encapsulate PUFAs-rich oil in an earlier paper (Zhang, Wang, et al., 2023). The microcapsules produced using (SPC-MD conjugate)-CG coacervates exhibited significantly enhanced stability against oxidation, compared to the microcapsules produced using (SPC-MD mixture)-CG coacervates (Zhang, Wang, et al., 2023). It was due to the robust microcapsule walls formed by the conjugate-based coacervates. It was hypothesised that this structure would be able to keep the integrity of microcapsules in the gastric environment and release the encapsulated oil in the intestinal environment. Therefore, in this study, we aimed to advance the science further by investigating the *in-vitro* digestion canola oil microcapsules stabilised by (SPC-MD conjugate)-CG coacervates. The complex coacervates produced using unconjugated mixture of SPC and MD and CG were used to produce the microcapsules of canola oil and were used to compare their digestion performance. The degradation of wall matrix, release of oil and lipolysis of the released oil were quantified using an established (INFOGEST international consensus) *in-vitro* digestion method.

2. Materials and methods

2.1. Materials

Spirulina powder (Bioglan Pty Ltd., New South Wales, Australia) was purchased from a local Chemist Warehouse outlet (Melbourne, Australia). Maltodextrin (MD) with a dextrose equivalence (DE) of 39 (GLUCIDEX® 39) and λ-carrageenan (CG) (GENUVISCO® CSW-2, Lambda) was kindly provided by Roquette Pty Ltd. (Lestrem, France). Canola oil was purchased from the local market. Transglutaminase (TG) Sprinkle Powder (Activa KS-LS) was purchased from Melbourne Food Depot (Melbourne, Australia). Alpha amylase (from human salivary 300–1500 units per mg protein, A1031), pepsin from porcine gastric mucosa (>2500 units per mg protein, P7012), bile extract from porcine (B8631), pancreatin from porcine pancreas (8 × USP specifications, P7545) were purchased from Sigma-Aldrich Pty Ltd. (New South Wales, Australia). This pancreatin was composed of amylase, trypsin, lipase, ribonuclease and protease. All other chemicals used in this study, including hydrochloric acid, sodium hydroxide, *n*-hexane and methanol, were purchased from Sigma-Aldrich Pty Ltd. (New South Wales, Australia). All of the above-mentioned chemicals were of analytical grade and were used as received.

2.2. Extraction of Spirulina protein and preparation of SPC-MD conjugates

The process used for the extraction of *Spirulina* protein concentrate (SPC) and preparation of SPC-MD conjugates were reported in our previous study (Zhang, Holden, et al., 2023). In brief, *Spirulina* powder was dispersed in the Milli Q water at a powder-to-water ratio of 1:15 (w/w). The pH of the dispersion was adjusted to 10.0 using 1 M NaOH. The dispersion was stirred at room temperature for 2 h and then centrifuged at 9000×*g* and 4 °C for 30 min. The supernatant was collected and adjusted to pH 3.5 using 1 M HCl and then centrifuged at 9000×*g* and 4 °C for 30 min. The protein precipitate was re-dispersed with Milli Q water and neutralised using 0.1 M NaOH, followed by freeze drying at 10 Pa and −80 °C (VaCo 10, ZIRBUS technology GmbH, Harz, Germany) for 48 h. The SPC powder was vacuum sealed and stored at 4 °C before use. The SPC extracted in this work had 78.9 ± 0.9% protein, 1.9 ± 0.6% lipid, 3.9 ± 0.1%, moisture and 4.1 ± 1.0% ash, measured by Kjeldahl method, AOAC Method No. 920.85, and AOAC Method No. 925.10, respectively.

SPC-MD conjugates were prepared by following the process reported previously (Zhang, Holden, et al., 2023). Briefly, SPC and MD were mixed at a ratio of 1:1 (w/w) and dispersed in the Milli Q water at a polymer-to-water ratio of 1:9 (w/w). The pH of the mixture was adjusted to 10.0 using 1 M NaOH, followed by agitation at 300 rpm and 4 °C overnight to allow complete hydration. The mixture was agitated and incubated at 60 °C for 6 h using a preheated shaking bath to induce the SPC-MD conjugation via the wet-heating route. Samples were collected

after 6 h heating, followed by a rapid cooling in an ice-water bath to stop the reaction. The pH of the reacted mixture was adjusted to 7.0 using 1 M HCl and then dialysed against water using a dialysis bag with a cut-off molecular weight of 3–5 kDa for 10 h to remove the unreacted MD. The SPC-MD conjugates was finally freeze-dried at 10 Pa and −80 °C for 48 h. This SPC-MD conjugate powder was vacuum sealed and stored at 4 °C before use.

2.3. Formation of SPC-MD-CG complex coacervates and encapsulation of oil

Canola oil was microencapsulated using (SPC-MD conjugates)-CG coacervates as wall material (Zhang, Wang, et al., 2023). Briefly, canola oil (5.21 g) was individually homogenised with 250 g SPC-MD conjugate or SPC-MD mixture (SPC:MD ratio of 1:1, w/w) solution using a high-speed laboratory homogeniser (Ultra-Turrax T-50 Homogeniser, IKA-Werke, Staufen, Germany) at 12,000 rpm for 4 min. The formed coarse oil-in-water (O/W) emulsions were further homogenised using a two-valve homogeniser (GEA Niro Soavi, PandaPLUS 2000, Düsseldorf, Germany) at 60 MPa for 3 passes to obtain fine emulsions. Then, 250 g CG dispersion (0.25%, w/w) was slowly added into the O/W emulsion and the mixture was agitated at 800 rpm and 40 °C. The pH of the mixed emulsion was adjusted to 3.0 using 1 M HCl to induce complex coacervation. The liquid microcapsules were cooled down to 5 °C under the agitation of 800 rpm and crosslinked by adding 50 mL 2% (w/w) transglutaminase solution. These emulsions were heated to 25 °C to activate the enzyme and agitated for 5 h to allow complete crosslinking. Finally, the crosslinked liquid microcapsules were spray dried using a laboratory-scale Mini Spray Dryer (Büchi Corporation, New Castle, DE, USA) equipped with a twin-fluid atomising nozzle (d = 0.5 mm diameter). The inlet and outlet temperature of the drying air were set at 170 °C and 90 ± 2 °C, respectively. These microcapsule powders were packed and stored at 4 °C until further use.

2.4. In-vitro digestion of microcapsules

Simulated salivary fluid (SSF), simulated gastric fluid (SGF), and simulated intestinal fluid (SIF) were prepared following INFOGEST protocol (Brodkorb et al., 2019) with minor modifications (Table 1).

2.4.1. Simulated oral digestion

Briefly, 2.0 g microcapsules were mixed with 5.0 mL of Milli Q water and 3.5 mL SSF was added. Then, $CaCl_2$ and α-amylase were added to the mixture to achieve 0.75 mM concentration and 75 U mL^{-1} activity, respectively. The total volume of mixture was then adjusted to 10 mL using Milli Q water. Its pH was adjusted to 7.0 with 1.0 M NaOH. The final mixture was agitated at 100 rpm and 37 °C for 2 min to complete the oral digestion.

2.4.2. Simulated gastric digestion

Ten mL of oral digestion digesta was mixed with 7.5 mL of SGF at 37 °C. $CaCl_2$ and porcine pepsin were added to achieve 0.075 mM concentration and 2000 U mL^{-1} activity, respectively in the final mixture. Milli Q water was added to make 20 mL volume of the total gastric mixture. The pH was adjusted to 3.0 with 1.0 M HCl and the final mixture was agitated at 100 rpm and 37 °C for 2 h to complete the gastric digestion.

2.4.3. Simulated intestinal digestion

Fifteen mL of SIF was added to 20 mL of gastric digesta at 37 °C, followed by adding pancreatin, bile salt and $CaCl_2$ to achieve 100 U mL^{-1} of trypsin activity, 10 mM of bile salt concentration and 0.3 mM of $CaCl_2$ concentration in the final mixture, respectively. Milli Q water was added to achieve 40 mL volume of intestinal mixture. The pH was adjusted to 7.0 with 1.0 M NaOH and the final mixture was agitated at 100 rpm and 37 °C for 2 h to complete the intestinal digestion.

2.5. Particle size and zeta potential of digesta

The particle size of the microcapsules was measured in the course of *in-vitro* digestion using a dynamic light scattering method (Mastersizer 3000, Malvern Instruments Ltd., Malvern, UK). Samples were diluted in recirculating water by agitating at 200 rpm. The refractive indices of the particle and dispersant were set at 1.52 and 1.33, respectively. Zeta potential of the digesta was measured using a Zetasizer (Nano-ZS, Malvern Instruments Ltd., Malvern, UK). The digesta samples were diluted 500 times prior to each measurement using Milli Q water and the pH of the diluted sample was adjusted to match that of the undiluted digesta (3.0 or 7.0).

2.6. Degree of hydrolysis of protein

The degree of hydrolysis of spirulina protein, present as part of the microcapsule wall, during digestion was determined using the *o*-phthaldialdehyde (OPA) spectrophotometric assay, according to Nielsen et al.'s (2001). Briefly, 80 mg of OPA was dissolved in 2 mL of methanol and mixed with 50 mL of borax buffer (0.1 M, pH 9.7), 5 mL of 20% (w/w) sodium dodecyl sulfate (SDS) solution and 0.2 mL of β-mercaptoethanol. The volume of the solution (OPA reagent) was adjusted to 100 mL with Milli Q water. During the *in-vitro* digestion, 40 μL of samples were collected at 0, 15, 30, 60, 90 and 120 min and mixed with 2.0 mL of OPA reagent. The mixture was incubated at 35 °C for 2 min. Then the absorbance at 340 nm of the mixture was measured using a UV–Vis spectrometer (Lambda 35, PerkinElmer Pty. Ltd., Waltham, MA, USA) to determine the free NH_2 group content in the samples. A calibration curve ($y = 0.0467x + 0.2337$, $R^2 = 0.999$) was established using 0–10 mM standard solutions of L-leucine.

2.7. Molecular weight of protein

The level of hydrolysis of spirulina protein, present in the microcapsule wall, was determined by measuring the change of its molecular weight. Sodium dodecyl sulfate polyacrylamide gel electrophoresis (SDS-PAGE) was used under reducing condition (Laemmli, 1970). For

Table 1
The composition of electrolyte stock solutions used to prepare simulated digestion fluids. The total volume of each simulated fluid was adjusted to 500 mL by diluting with Milli Q water. SSF = simulated salivary fluid, SGF = simulated gastric fluid and SIF = simulated intestinal fluid.

Types of salt	Stock concentration (M)	SSF (pH 7.0)	SGF (pH 3.0)	SIF (pH 7.0)
		Final concentration (mM)	Final concentration (mM)	Final concentration (mM)
KCl	0.5	15.1	6.9	6.8
KH_2PO_4	0.5	3.7	0.9	0.8
$NaHCO_3$	1	13.6	25	85
NaCl	2	–	47.2	38.4
$MgCl_2(H_2O)_6$	0.15	0.15	0.12	0.33
$(NH_4)_2CO_3$	0.5	0.06	0.5	–
HCl	6	1.1	15.6	8.4

this propose, the digesta samples collected at oral phase and 15, 30, 60, 90 and 120 min of the gastric and intestinal phase were used. Briefly, a 4–12% precast polyacrylamide gel containing 4% stacking gel and 12% separation gel was applied in a Mini-PROTEAN Tetra Cell (Bio-Rad, Mini-Protein apparatus III). The collected and diluted sample solution (1%, w/v) was mixed with loading buffer (95% 2 × Laemmli buffer and 5% β-mercaptoethanol, w/w) at a sample-to-buffer ratio of 3:1 (v/v). The mixture was heated at 100 °C for 10 min. Ten μL sample was loaded into the precast gel and the electrophoresis was performed in a Tris-glycine running buffer (pH 8.3). The SDS-PAGE test was run at 110 V for 60–80 min until the dye front reached the reference line. Finally, the gel was stained with Coomassie Brilliant Blue R-250 dye for 60 min and destained with a decolorization solution composed of 10% (v/v) methanol and 10% (v/v) acetic acid by three times. The gel image was acquired and analysed using Image Lab (Bio-Rad, Hercules, CA, USA).

2.8. Observation of microstructure of microcapsules and digesta

2.8.1. Scanning electron microscopy

The overall microstructure of the microcapsule was studied using a scanning electron microscope (SEM) (FEI Quanta 200 ESEM, Japan). Briefly, 1 mL of digesta was collected at the end of oral, gastric and intestinal phase and freeze-dried at −80 °C under a vacuum pressure of 10 Pa for 48 h. The resulting powder was coated with palladium using a Sputter Coater (VG Microtech, England). The images were captured under magnification of 5000× and an accelerating voltage of 10 kV.

2.8.2. Optical microscopy

During *in-vitro* digestion, one drop of the digesta at the end of each digestion stage was collected and transferred to microscope slides to monitor their morphology change. An optical microscope (Leica 108, Heidelberg, Germany) was used for this purpose at 40× magnification.

2.8.3. Confocal scanning laser microscopy

A confocal scanning laser microscope (CLSM) (Nikon Co. Ltd., Tokyo, Japan) was used to visualise the release of oil during digestion, according to Rafe et al. (2012) with a minor modification. Briefly, 1 mL of the digesta was collected at the end of each stage of digestion and mixed with 10 μL of 0.1% (v/v) Nile red solution and 10 μL of 0.1% (v/v) fluorescein isothiocyanate (FITC) to stain the oil and protein, respectively. These mixtures were then left in the dark for 1 h before CLSM scan. Images were captured with a 40 × objective (oil immersion, numeric aperture 1.30). The laser excitation wavelengths were selected as 488 nm and 512 nm for Nile red and FITC, respectively.

2.9. Oil release

The oil was extracted at the end of each digestion phase using organic solvent, according to Eratte et al. (2017) with a minor modification. Briefly, each digesta was mixed with 25 mL of hexane, followed by a 60 s vortex. After centrifugation at 6000×*g* and 20 °C for 15 min, the supernatant was filtered into a pre-weighted flask through a filter paper (Whatman No.1). The extraction process was repeated for three times. Then, the filtrate was combined, and the solvent was evaporated using a rotary evaporator. The extracted oil was heated at 80 °C for 1 h to remove the residual solvent then cooled down to room temperature. The amount of released oil in the digestion process was calculated using Equation (1).

$$\text{Released oil } (\%) = \frac{\text{Mass of oil released from microcapsules (g)}}{\text{Total mass of oil in microcapsules (g)}} \times 100. \quad (1)$$

2.10. Lipolysis of released oil

The lipolysis of the released oil during intestinal digestion was studied by measuring release of fatty acids (FFAs), as described by Li and McClements (2011). During the intestinal digestion, an automatic titration unit (stat 842 Titrando, Metrohm Ltd, Herisau, Switzerland) was used to maintain the pH of the digesta at 7.0 by using 0.1 M NaOH. The volume of consumed NaOH solution was recorded to calculate the released FFA. It was assumed that two molecules of FFAs were released from one totally digested triglyceride molecule, and 2 mol of NaOH were theoretically required to neutralise 1 mol of triglyceride (Li & McClements, 2010). The content of released FFA was calculated using Equation (2).

$$\text{FFA } (\%) = 100 \times \left(\frac{V_{NaOH} \times m_{NaOH} \times M_{lipid}}{W_{lipid} \times 2} \right). \quad (2)$$

where, V_{NaOH} is the volume of 0.1 M NaOH required to neutralise released FFA (mL), m_{NaOH} is the molarity of NaOH (0.1 M), W_{lipid} is the total mass of oil present in the digestion system (g) and M_{lipid} is the molecular weight of the canola oil (876.6 g/mol).

The release profile of FFA as a function of time (FFA_t) was represented with a first-order reaction kinetics model, shown in Equation (3) (Joyce et al., 2018).

$$FFA_t = FFA_{max}\left(1 - e^{-kt}\right). \quad (3)$$

where, FFA_{max} is the maximum value of total FFA level (%), k is the constant of first-order reaction kinetics (min^{-1}) and t is the digestion time (min).

2.11. Statistical analysis

All the experiments were carried out in triplicate unless mentioned otherwise. The results are expressed as mean ± standard deviation. The data analysis was performed using SPSS statistical software (SPSS 23.0, IBM, Armonk, NY, USA). Significant differences between any two mean values were analysed using one-way analysis of variance (ANOVA) with Duncan test at a 95% confidence level ($p < 0.05$).

3. Results and discussion

3.1. Particle size of digesta

The distribution of particle of the undigested microcapsules and digesta of oral, gastric, and intestinal stages are presented in Fig. 1 and their mean values ($D_{4,3}$) are presented in Table 2. The canola oil microcapsules stabilised using (SPC-MD mixture)-CG coacervates had larger particle size than the one stabilised using (SPC-MD conjugate)-CG coacervates. The smaller size was due to the improved emulsifying and encapsulating properties of conjugate, compared with the original protein. In our previous work, SPC-MD conjugates showed higher solubility and more flexible structure than SPC (Zhang, Holden, et al., 2023). The conjugates also migrated and adsorbed at the O/W interface faster to form a robust and thick viscoelastic layer around emulsion droplets (Lv et al., 2023; Razavi et al., 2021; Zhang, Liao, et al., 2021; Zhang, Yue, et al., 2021). Thus, the microcapsules with conjugate-based coacervates as wall material had a more compact structure than the one stabilised by mixture-based coacervates (Zhang, Wang, et al., 2023).

At the end of oral digestion, no significant change was observed in the particle size and distribution of the digesta compared to that of undigested microcapsules (Table 2, Fig. 1). Since the oral phase was short (2 min), this time frame was not sufficient to erode the microcapsule wall and induce the flocculation and coalescence of droplet and thus increase the particle size of the digesta (Timilsena et al., 2017).

At the end of gastric digestion for 2 h, the mean particle size of both microcapsules stabilised by (SPC-MD mixture)-CG coacervates and (SPC-MD conjugate)-CG coacervates increased (Table 2). Additionally, there was a shift in the particle size distribution towards larger size (≥10 μm) (Fig. 1a and b). It was primarily due to breakdown of protein by pepsin in the gastric environment (Rahmani-Manglano et al., 2022).

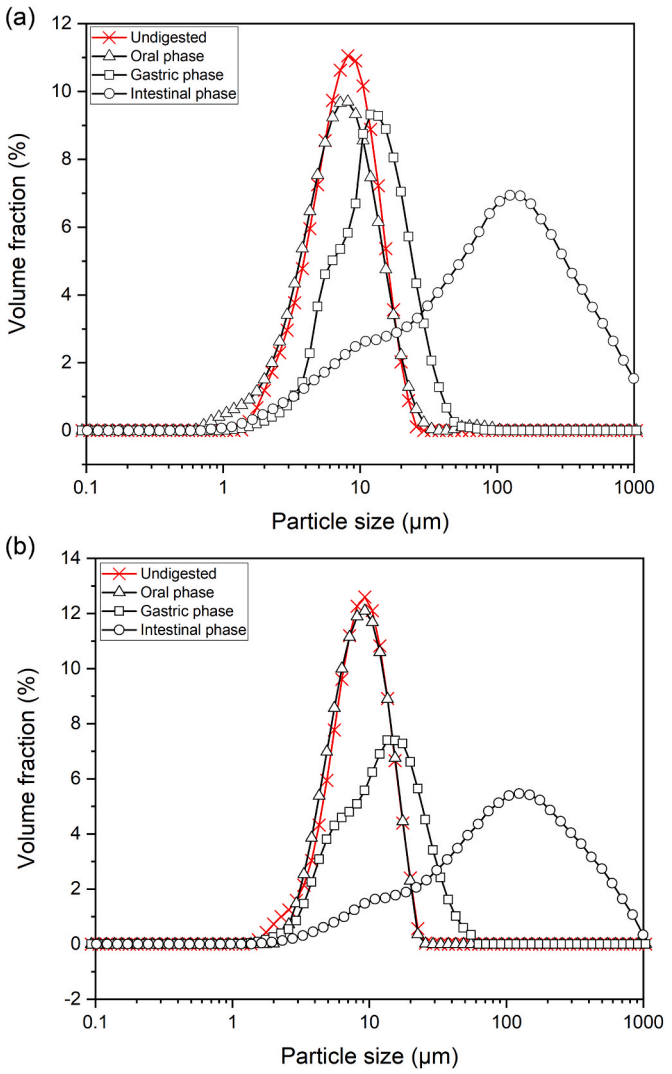

Fig. 1. Particle size distributions of microcapsules before and during in-vitro digestion: (SPC-MD mixture)-CG coacervates microcapsule (a) and (SPC-MD conjugate)-CG coacervates microcapsule (b).

Table 2
Mean droplet size ($D_{4,3}$) of microcapsules (undigested) and digesta of obtained at the end of oral, gastric and intestinal digestion. (SPC-MD mixture)-CG-CO = Canola oil microcapsules produced using (SPC-MD mixture)-CG coacervates; (SPC-MD conjugate)-CG-CO = Canola oil microcapsules produced using (SPC-MD conjugate)-CG coacervates.

Sample	Undigested sample $D_{4,3}$ (μm)	Digested sample $D_{4,3}$ (μm)		
		Oral phase	Gastric phase	Intestinal phase
(SPC-MD mixture)-CG-CO	9.14 ± 0.05^{a}	9.48 ± 0.13^{a}	11.12 ± 0.31^{a}	195.9 ± 8.01^{a}
(SPC-MD conjugate)-CG-CO	8.39 ± 0.04^{b}	8.86 ± 0.07^{b}	10.37 ± 0.28^{b}	179.7 ± 6.04^{b}

Note: The different letters in superscript within a column indicate statistically significant differences ($p < 0.05$) by Duncan's multiple range test.

The wall materials underwent partial hydrolysis, which led to the release of the oil and coalescence of oil droplets (discussed further in section 3.6), thereby increasing their size. However, the microcapsules formed using conjugate-based coacervates as wall materials still exhibit smaller particle sizes. This could be attributed to the conjugates' ability as wall material, which exerted stronger steric repulsions and enhanced the stability of oil droplets against flocculation and coalescence during gastric digestion (Nooshkam & Varidi, 2020). At the end of the intestinal digestion of 2 h, the mean particle size of digesta of both microcapsules increased significantly (Table 2). The main peak of the particle size distribution (of the intestinal digesta) shifted towards the large size region (≥100 μm). This could be attributed to the aggregation and coalescence of oil droplets caused by further hydrolysis of the protein by trypsin in the pancreatin (Zhang, Liao, et al., 2021; Zhang, Yue, et al., 2021). Notably, the particle size of digesta of microcapsules stabilised using (SPC-MD conjugate)-CG coacervates as wall materials were significantly smaller than that of microcapsules stabilised by (SPC-MD mixture)-CG coacervates during digestion. The conjugate-based coacervates are known to create a relatively thick and compact layer around oil droplets compared with the mixture-based one (Xu et al., 2014). The resulting compact wall of microcapsules was expected to slow down the ingress of digestive fluids and enzymes and thus slow down the rupture of the wall.

3.2. Zeta-potential of digesta

The zeta-potential of the digesta at the end of oral, gastric and intestinal phase digestion are shown in Fig. 2. The digesta of both microcapsules were negatively charged at the end of oral digestion. The negative values of zeta potential of both digesta were expected as the pH 7.0 of SSF was higher than the isoelectric point of both SPC-MD mixture and conjugate (pI = 3.5–3.6). This was because the amino acids of protein component become negatively charged at neutral pH (Ardestani et al., 2022; Hasanvand et al., 2018). In addition, CG also contributed to the negative charge at pH 7 (Zhang, Wang, et al., 2023). As the figure shows, the magnitude of the zeta potential of the digesta of conjugate-based microcapsules was higher than that of mixture-based ones. It could be due to the attachment of negatively charged MD molecules to SPC and the consumption of positively charged amino acids during conjugation (Zhang, Holden, et al., 2023).

The absolute zeta-potential values of digesta of both microcapsules decreased at the end of gastric phase (Fig. 2) due to acidic environment

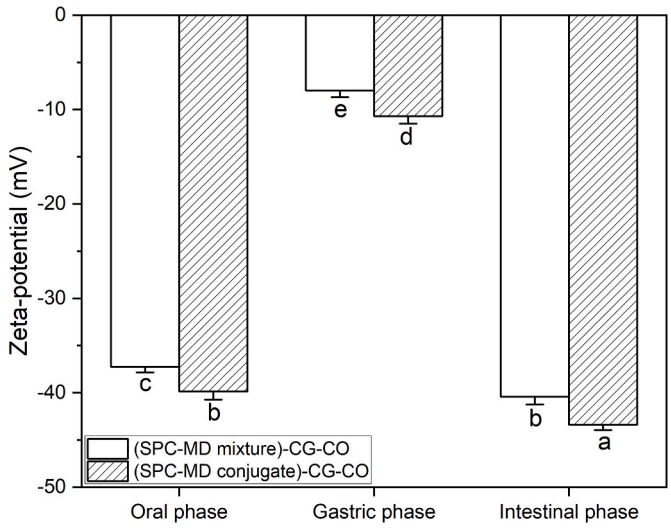

Fig. 2. Zeta-potential of (SPC-MD mixture)-CG and (SPC-MD conjugate)-CG coacervates microcapsule at the end of oral, gastric and intestinal digestion. (SPC-MD mixture)-CG-CO = Canola oil microcapsules produced using (SPC-MD mixture)-CG coacervates; (SPC-MD conjugate)-CG-CO = Canola oil microcapsules produced using (SPC-MD conjugate)-CG coacervates.
Note: Different letters above each value indicated significant differences ($p < 0.05$) by the Duncan's multiple test.

(pH 3.0). This reduction of magnitude of zeta potential (decrease of charge density of negative charge) due to the pH of environment being lower than the pI of SPC as its conjugates (with MD) and coacervates (with CG). This could also be due to the presence of other charged compounds such as polysaccharides and pepsin (pI = 1) (Rahmani--Manglano et al., 2022). At the end of the intestinal digestion for 2 h, the digesta of both microcapsules became more negatively charged. These absolute zeta-potential values of intestinal digesta were even higher than those obtained at the oral phase. This was because both SPC-MD mixture and conjugate exhibited a negative charge in this neutral pH environment. Moreover, the free fatty acid produced during the lipolysis were also known to be negatively charged (Section 3.7), contributing to the increased negative charge (Ni et al., 2021; Rahmani-Manglano et al., 2022).

In the entire *in-vitro* digestion process, the digesta of microcapsules stabilised by conjugate-based coacervates always showed higher absolute zeta-potential values than the ones stabilised mixture-based coacervates. This indicated that the conjugates based complex coacervates exerted higher electrostatic repulsion on the digeata droplets and reduced droplet aggregation. This result further explained the reaction behind small particle size of digesta of microcapsules stabilised by conjugate-based complex coacervates (Section 3.1).

3.3. Proteolysis of microcapsules and digesta

The proteolysis of microcapsules was measured in terms of free amino acid content (Fig. 3). As can be observed, proteolysis did not occur in the oral phase. At the end of gastric phase, NH_2 concentration in both microcapsules increased close to 11 mM within the first 15 min. Then it increased gradually until the end of gastric digestion. The amount of free amino acid groups produced during the entire gastric digestion phase was found to be lower compared to the amount generated during the intestinal phase. This was because pepsin played an important role in breaking down the peptide bonds between large protein components, converting them into polypeptides (Gong et al., 2022). There was no significant difference between NH_2 values of digesta obtained from both types of microcapsules during gastric digestion ($p > 0.05$). This finding implied that the utilisation of both conjugate- and mixture-based coacervates as wall materials conferred comparable protection to microcapsules against gastric digestion.

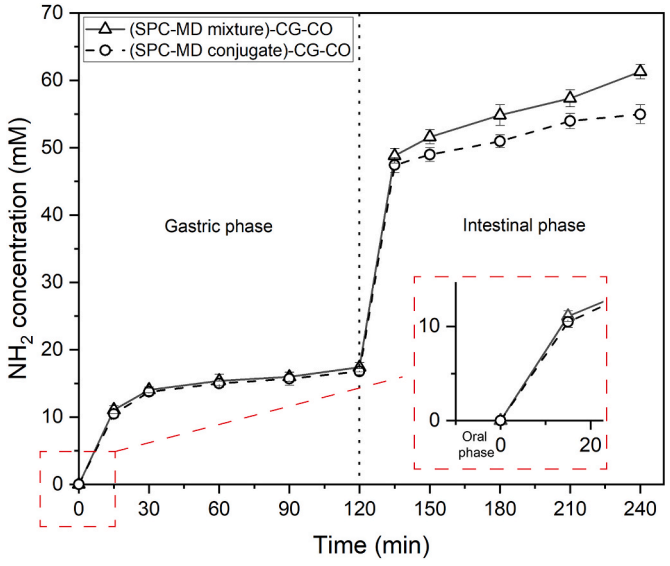

Fig. 3. The free amino acid groups (NH_2) concentration in the microcapsules during simulated digestion (0–120 min for gastric digestion and 120 to 240 for intestinal digestion, respectively). (SPC-MD mixture)-CG-CO = Canola oil microcapsules produced using (SPC-MD mixture)-CG coacervates; (SPC-MD conjugate)-CG-CO = Canola oil microcapsules produced using (SPC-MD conjugate)-CG coacervates.

In the intestinal phase, the concentration of NH_2 increased to about 55 and 61 mM in the microcapsule stabilised by the mixture- and conjugate-based coacervates (Fig. 3). This was due to the presence of both bile salts and pancreatin. The bile salts adsorbed at the surface layer and promoted the hydrolysis of proteins by pancreatin. The pancreatin which contained peptidases hydrolysed the protein into small peptides and amino acids (Li et al., 2023). The microcapsules produced using conjugate-based coacervates as wall materials had significantly lower content of free amino acid groups compared to those produced using mixture-based coacervates. This result was consistent with the variation of particle size and zeta-potential of digesta of both microcapsules during gastrointestinal digestion (section 3.1 and 3.2). The conjugate-based coacervates formed a thicker wall that retained the integrity of microcapsules during intestinal digestion for a longer period of time.

3.4. Reduction of molecular weight of wall materials during in-vitro digestion

The breakdown of wall microcapsules during digestion was analysed using reducing SDS-PAGE (Fig. 4). The undigested microcapsules, produced using SPC-MD mixture-based complex coacervates, showed molecular weight bands at approximately 10 kDa.This was consistent with our previous study where the extracted SPC exhibited a molecular weight range between 5.0 and 10.5 kDa, by MALDI-TOF-MS analysis (Zhang, Holden, et al., 2023). The undigested (SPC-MD mixture)-CG and (SPC-MD conjugate)-CG microcapsules showed significantly different SDS-PAGE bands, due to the molecular difference between conjugate and original protein. In our previous research, we reported a significant increase in the molecular weight of SPC after 6 h of Maillard conjugation. This was supported by the new peaks with increased molecular weights at approximately 11–16 KDa (Zhang, Holden, et al., 2023). The digesta obtained at the end of oral digestion of both microcapsules showed only one new band at about 60 kDa indicating the presence of α-amalyse (Fig. 4) (Bano et al., 2011). This observations suggested that the wall materials of both microcapsules remained intact during the oral phase.

Most of the initial molecular weight related bands of SPC disappeared within the first 15 min of the gastric digestion. New protein fractions with molecular weight below 15 kDa were formed due to proteolysis by pepsin (Gong et al., 2022). The molecular weight distribution of digesta of these two types of microcapsules remained virtually unchanged throughout the entire gastric stage, indicating their ability to resist further proteolysis. The molecular weight of protein fractions present in the digesta of conjugate-based microcapsules was higher (25–35 kDa) compared to those present in the digesta of mixture-based conjugates. These observations suggested that the wall of microcapsules created using conjugate-based complex coacervates of SPC exhibited enhanced proteolytic resistance.

During the intestinal digestion, the digesta of microcapsules produced using mixture- and conjugate-based complex coacervates had similar molecular weight bands, ranging from 20 to 55 kDa. The bands observed at higher positions than those of gastric digesta were attributed to pancreatin (Fig. 4) (Gao et al., 2021). Notably, most protein fractions with a molecular weight below 15 kDa disappeared due to further hydrolysis of the protein fractions by pancreatic proteases into small peptides and amino acids (Li et al., 2023). This observation was consistent with the results presented in Section 3.3, that the rapid hydrolysis of protein and rapid increase of NH2 concentration occurred within the initial 15 min of intestinal digestion. In Hu et al. (2022)'s study, the authors observed that the characteristic bands of β-lactoglobulin rapidly disappeared during the intestinal digestion due to the proteolysis by pancreatic trypsin.

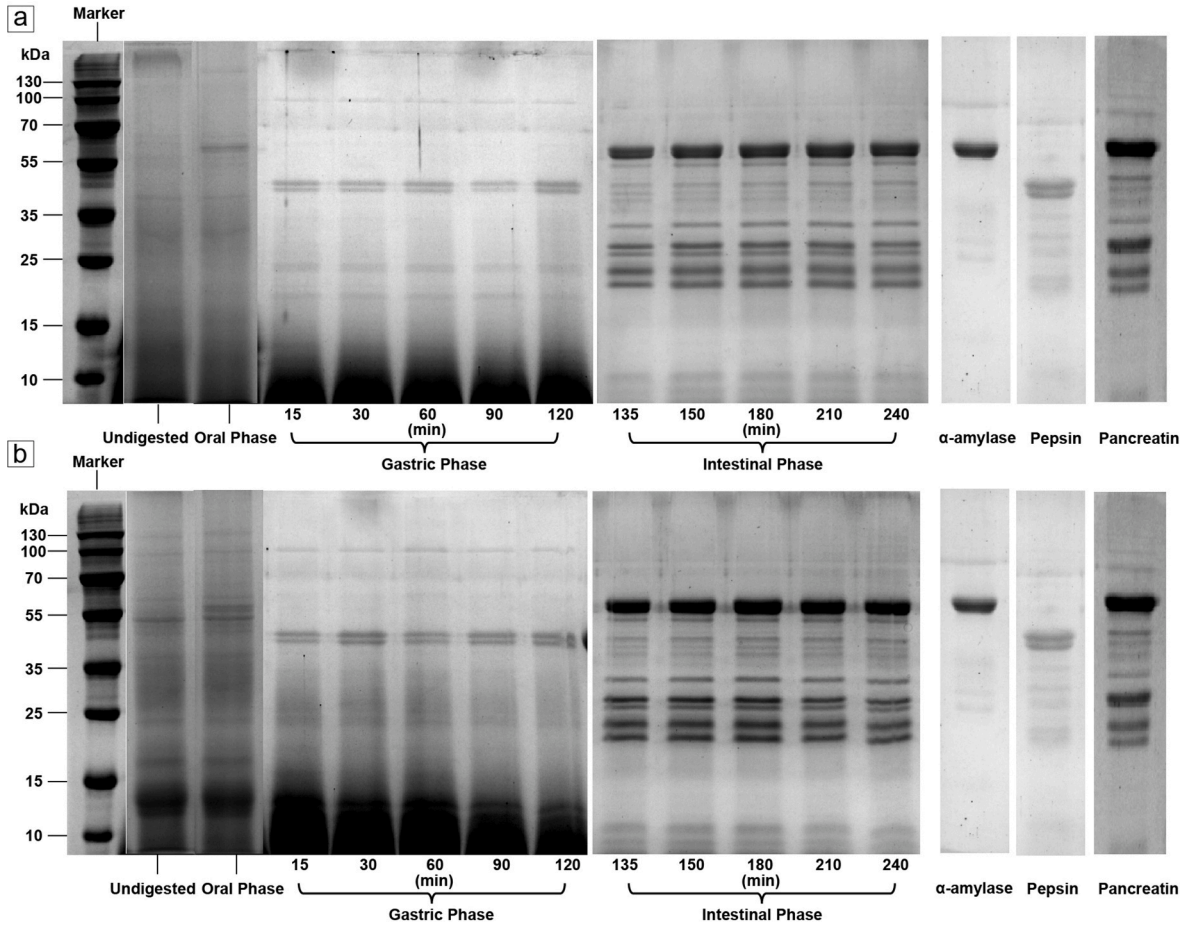

Fig. 4. SDS-PAGE of microcapsules (a: (SPC-MD mixture)-CG and b: (SPC-MD conjugate)-CG as wall material) before and during in-vitro digestion.

3.5. *Microstructure of digesta*

The images of digesta obtained from SEM and optical microscopes at the end of each digestion stage are presented in Figs. 5 and 6, respectively. The undigested canola oil microcapsules stabilised by (SPC-MD mixture)-CG and (SPC-MD conjugate)-CG coacervates showed similar spherical shapes without any cracks (Fig. 5a and e).

The microstructure of digesta of both microcapsules at the end of oral phase was similar and was unaltered as shown by SEM images which corroborated the results of SDS-PAGE (Fig. 4). The digesta of both microcapsules retained their original spherical shape in the gastric environment (Fig. 5c and g). The distinctly different morphology of undigested microcapsules (Fig. 6a and e) compared to orally digested ones (Fig. 6b and f) cased by swelling due to SSF and also due to the change of pH environment from acidic (3.5 of coacervates) to neutral (7.0 of SSF) which was expected to weaken the coacervates. The optical microscopic images of gastric digesta revealed some degree of aggregation of the microcapsules into clumps (Fig. 6c and g) most probably due to partial hydrolysis of SPC by pepsin, as explained in section 3.1.

The original morphology of microcapsules disappeared completely in the intestinal digesta (Fig. 5d and h), indicating strong proteolytic degradation of SPC by pancreatic enzymes and consequent degradation of microcapsule structure. An uneven and rough surface was observed in the SEM images, due to the presence of polysaccharides (Gao et al.,

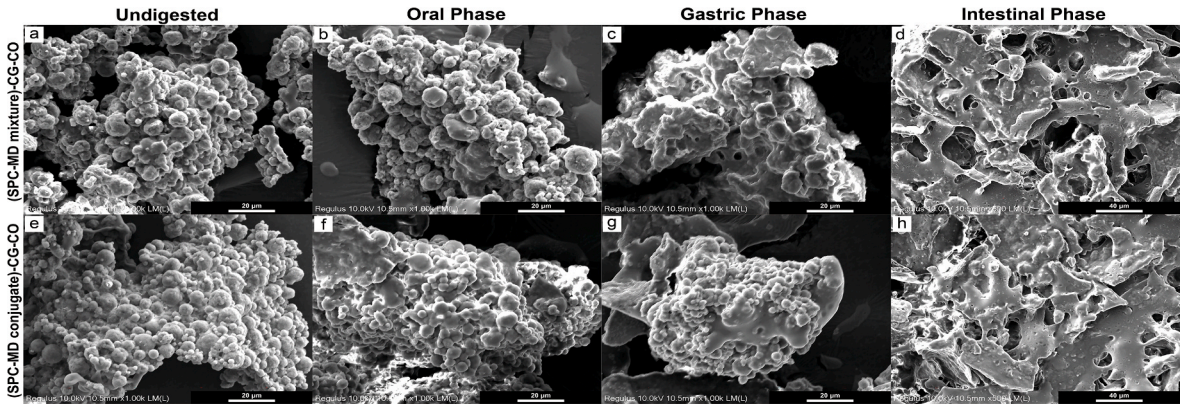

Fig. 5. SEM images of microcapsules (a–d: (SPC-MD mixture)-CG coacervates and e–h: (SPC-MD conjugate)-CG coacervates as wall material).

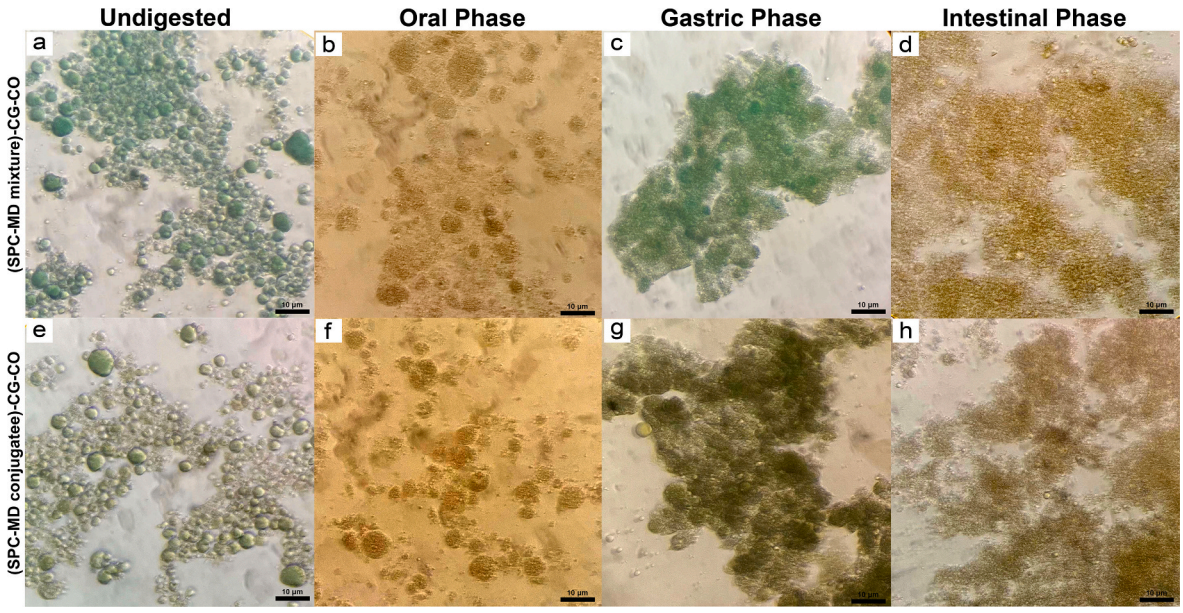

Fig. 6. Optical microscope images of microcapsules before and after simulated digestion. (a–d): (SPC-MD mixture)-CG coacervates and (e–h): (SPC-MD conjugate)-CG coacervates as wall material.

2021). In addition, droplets with an increased mean particle size were found in the digesta. The optical microscopic images further confirmed the hydrolysis of microcapsules during intestinal digestion (Fig. 6d and h). The level of aggregation observed in the microcapsules found in the intestinal digesta was lower in comparison to the microcapsules found in the gastric digesta (Fig. 6c, g and 6d, 6h). This could be attributed to the higher level of protein hydrolysis, weakening of wall structure and loosening of aggregates (Li et al., 2022).

3.6. Release of oil

The CLSM images of undigested microcapsules and digesta obtained at the end of each digestion stage and release oil content are presented in Figs. 7 and 8a, respectively. The canola oil microcapsules stabilised by (SPC-MD mixture)-CG and (SPC-MD conjugate)-CG coacervates showed uniform droplet distributions at the end of oral digestion (Fig. 7a and d) and they also preserved their structural integrity. In this digestion phase,

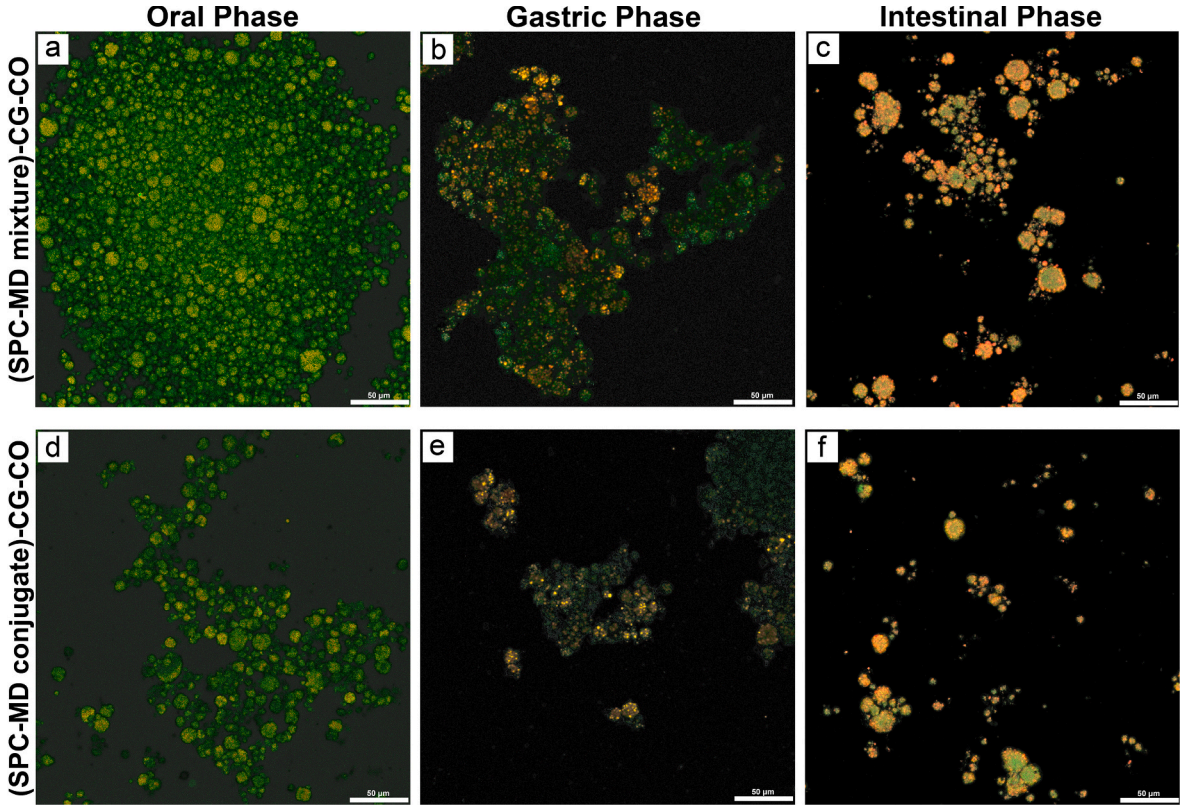

Fig. 7. CLSM images of digested microcapsules at the end of oral, gastric and intestinal digestions. (a–c): (SPC-MD mixture)-CG coacervates and (d–f): (SPC-MD conjugate)-CG coacervates as wall material.

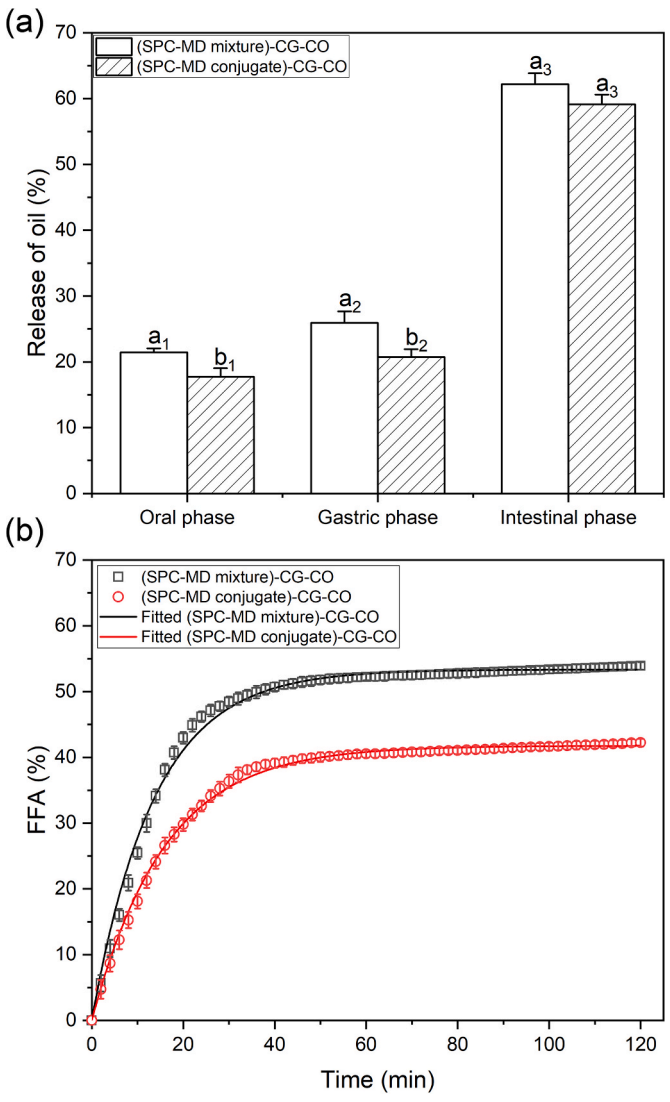

Fig. 8. Release of oil from digested microcapsules at the end of oral, gastric and intestinal digestion (a) and the released free fatty acids (FFAs) from digested microcapsules as a function of time during the intestinal digestion (solid lines indicate the fitted curves) (b).
Note: Different lowercase letters with the same subscripts above each value indicated significant differences ($p < 0.05$) by the Duncan's multiple test.

21.5 and 17.7% of encapsulated oil was released from the mixture-based and conjugate-based coacervates microcapsules, respectively (Fig. 8a). The oil released in the oral stage was unentrapped surface oil (Zhang, Wang, et al., 2023).

At the end of gastric stage, the released oil content slightly increased in both microcapsules (Fig. 8a). The CLSM images also showed increased droplet aggregation and the intensity of red colour (indicator of oil) was also increased in both microcapsules, even though their microstructure was not disrupted (Fig. 7b and e). This could be due to the partial hydrolysis of SPC component of the wall by pepsin, which released small amount of oil (Ni et al., 2021). Notably, the conjugate-based coacervate microcapsules released less oil than mixture-based coacervate microcapsules. It further confirmed that the microcapsule wall material synthesised using covalently bonding the SPC with MD was more resistant to gastric digestion. The lesser amount of oil release from the microcapsules produced using conjugate-based coacervates as wall material might be attributed to protein-polysaccharide conjugation, which caused protein unfolding and amino acid consumption through covalently bonding with carbonyl groups of reducing carbohydrates (Zhang, Holden, et al., 2023). This reduced the number of digestion sites, specifically lysine residues, thereby reducing the ability of pepsin in hydrolysing the protein (Lin et al., 2013; Niu et al., 2016). This ultimately increased the resistance of conjugate to pepsin digestion.

The release of the encapsulated oil in the intestinal phase from the mixture- and conjugate-based coacervate microcapsule was 62 and 67%, respectively (Fig. 8b). The intensity of red colour increased further in CLSM images of intestinal digesta (Fig. 7c and f). This observation was in line with the proteolysis of microcapsule wall materials during intestinal digestion (Figs. 3 and 4). Wang et al. (2018) studied the release behaviour of peony seed oil stabilised in a whey protein isolate-corn syrup-soy lecithin matrix. The authors observed that the oil content released at the end of intestinal phase was similar to that found in this study. At the end of intestinal digestion, the released oil contents of the canola oil microcapsules stabilised by (SPC-MD mixture)-CG and (SPC-MD conjugate)-CG coacervates were not significantly different (Fig. 8a). Overall, conjugate-based coacervates, as wall material, were effective in protecting the encapsulated oil in gastric phase and releasing it in the subsequent intestinal phase.

3.7. Lipolysis of oil

The lipolysis of oil released in the intestinal phase was measured using free fatty acids (FFAs) content of the released oil (Fig. 8b). The release kinetics of FFAs fitted using a first-order reaction (Eq. (3)) (solid lines, Fig. 8b). The kinetic parameters, including FFA_{max}, k values and $t_{1/2}$ were calculated (Table 3). In both microcapsules produced with (SPC-MD mixture)-CG and (SPC-MD conjugate)-CG coacervate, a significantly increased FFA content was observed in the first 20 min of intestinal digestion. The presence of lipase in pancreatin was the primary factor contributing to the fast adsorption of lipase at the oil/water interface, which facilitated the hydrolysis of oils into FFAs (Hur et al., 2009). The rate of lipolysis rate decreased gradually with the progress of digestion. This could be due to lipolytic products such as FFAs and monoglycerides hindered the access and adsorption of lipase at oil-in-water interface (Mat et al., 2020).

FFA_{max} and k values of lipolysis of conjugate-based microcapsules digesta were significantly lower than those of mixture-based microcapsules, indicating slower digestion of lipid encapsulated in conjugate-based coacervates of SPC. The $t_{1/2}$ value represents the time it takes to digest half of the released oil (Ni et al., 2021). The conjugate-based coacervate microcapsules exhibited longer $t_{1/2}$ value than the mixture-based ones (11 versus 9.4 min) confirming the slower lipolysis of encapsulated canola oil during intestinal digestion.

A decreased lipid digestion rate of nano-emulsions was reported by Fan et al. (2017) when whey protein isolate-dextrin conjugate was used as wall material, compared to when the whey protein was used by itself. The conjugate-based wall material formed a thick protective layer surrounding the encapsulated lipids. Thus, it slowed down the adsorption and action of the lipase (Fan et al., 2017; Nooshkam & Varidi, 2020). Overall, the (SPC-MD conjugate)-CG coacervates showed promising

Table 3
Kinetic parameters for the lipolysis of released oil during intestinal digestion. (SPC-MD mixture)-CG-CO = Canola oil microcapsules produced using (SPC-MD mixture)-CG coacervates; (SPC-MD conjugate)-CG-CO = Canola oil microcapsules produced using (SPC-MD conjugate)-CG coacervates.

Sample	FFA_{max} (%)	k (min^{-1})	$t_{1/2}$ (min)	R^2
(SPC-MD mixture)-CG-CO	53.35 ± 0.17[a]	0.074 ± 0.001[a]	9.4	0.993
(SPC-MD conjugate)-CG-CO	41.77 ± 0.09[b]	0.063 ± 0.005[b]	11	0.997

Note: t1/2 is the time required to achieve half lipolysis of the lipid.
The different letters in superscript within a column indicate statistically significant differences ($p < 0.05$) by Duncan's multiple range test.

properties as novel wall materials for the targeted delivery of unstable (canola) oil. Notably, the encapsulated oil was protected well before reaching the intestine where it was released and digested slowly.

4. Conclusion

This study investigated the effectiveness of complex coacervates formed by unconjugated and (maltodextrin)-conjugated *Spirulina* protein (SPC-MD conjugate) in protecting encapsulated canola oil during the gastric phase and facilitating its release in the intestinal phase. Carrageenan (CG) was used to generate the coacervates. Both microcapsules produced using unconjugated (SPC-MD mixture)-CG coacervate and conjugated (SPC-MD conjugate)-CG coacervate exhibited considerable stability during oral digestion. Only minor proteolysis of SPC occurred and the structure of microcapsule was preserved during gastric digestion, resulting in the release of surface oil only. However, in the intestinal phase, the structure of both microcapsules significantly degraded, leading to the release of 62–67% of the encapsulated oil, of which 40–55% underwent lipolysis. Notably, the conjugated SPC-based coacervates demonstrated a more robust wall structure compared to the unconjugated SPC-based coacervates, exhibiting slower breakdown of the structure, oil release, and lipolysis. These findings highlight the potential of complex coacervates formed by SPC, particularly when conjugated, as promising encapsulating wall materials for unstable oils, facilitating their delivery to the intestinal phase.

Author credit statement

Zijia Zhang: Conceptualization, Methodology, Writing—Original draft. Bo Wang: Conceptualization, Supervision, Writing – Reviewing and editing. Greg Holden: Conceptualization and Supervision. Chen Jie: Conceptualization and Supervision. Benu Adhikari: Conceptualization, Supervision, Writing – Reviewing and editing.

Declaration of competing interest

The authors declare that they have no known competing financial interests or personal relationships that could have appeared to influence the work reported in this paper.

Data availability

Data will be made available on request.

References

Ann Augustin, M., Sanguansri, L., Kartika Rusli, J., Shen, Z., Jiang Cheng, L., Keogh, J., & Clifton, P. (2014). Digestion of microencapsulated oil powders: In vitro lipolysis and in vivo absorption from a food matrix. *Food & Function, 5*(11), 2905–2912. https://doi.org/10.1039/C4FO00743C

Ardestani, F., Haghighi Asl, A., & Rafe, A. (2022). Phase separation and formation of sodium caseinate/pectin complex coacervates: Effects of pH on the complexation. *Chemical and Biological Technologies in Agriculture, 9*(1), 83. https://doi.org/10.1186/s40538-022-00355-7

Bannikova, A., Evteev, A., Pankin, K., Evdokimov, I., & Kasapis, S. (2018). Microencapsulation of fish oil with alginate: In-vitro evaluation and controlled release. *LWT, 90*, 310–315. https://doi.org/10.1016/j.lwt.2017.12.045

Bano, S., Qader, S. A. U., Aman, A., Syed, M. N., & Azhar, A. (2011). Purification and characterization of novel α-amylase from Bacillus subtilis KIBGE HAS. *AAPS PharmSciTech, 12*(1), 255–261. https://doi.org/10.1208/s12249-011-9586-1

Brodkorb, A., Egger, L., Alminger, M., Alvito, P., Assunção, R., Ballance, S., Bohn, T., Bourlieu-Lacanal, C., Boutrou, R., Carrière, F., Clemente, A., Corredig, M., Dupont, D., Dufour, C., Edwards, C., Golding, M., Karakaya, S., Kirkhus, B.Le Feunteun, S., … (2019). INFOGEST static in vitro simulation of gastrointestinal food digestion. *Nature Protocols, 14*(4), 991–1014. https://doi.org/10.1038/s41596-018-0119-1

Corrêa-Filho, L. C., Moldão-Martins, M., & Alves, V. D. (2019). Advances in the application of microcapsules as carriers of functional compounds for food products. *Applied Sciences, 9*(3), 571. https://doi.org/10.3390/app9030571

Dias, M. I., Ferreira, I. C. F. R., & Barreiro, M. F. (2015). Microencapsulation of bioactives for food applications. *Food & Function, 6*(4), 1035–1052. https://doi.org/10.1039/C4FO01175A

Donhowe, E. G., & Kong, F. (2014). Beta-carotene: Digestion, microencapsulation, and in vitro bioavailability. *Food and Bioprocess Technology, 7*(2), 338–354. https://doi.org/10.1007/s11947-013-1244-z

Eratte, D., Dowling, K., Barrow, C. J., & Adhikari, B. P. (2017). In-vitro digestion of probiotic bacteria and omega-3 oil co-microencapsulated in whey protein isolate-gum Arabic complex coacervates. *Food Chemistry, 227*, 129–136. https://doi.org/10.1016/j.foodchem.2017.01.080

Fan, Y., Yi, J., Zhang, Y., Wen, Z., & Zhao, L. (2017). Physicochemical stability and in vitro bioaccessibility of β-carotene nanoemulsions stabilized with whey protein-dextran conjugates. *Food Hydrocolloids, 63*, 256–264. https://doi.org/10.1016/j.foodhyd.2016.09.008

Gao, J., Liu, C., Shi, J., Ni, F., Shen, Q., Xie, H., Wang, K., Lei, Q., Fang, W., & Ren, G. (2021). The regulation of sodium alginate on the stability of ovalbumin-pectin complexes for VD3 encapsulation and in vitro simulated gastrointestinal digestion study. *Food Research International, 140*, Article 110011. https://doi.org/10.1016/j.foodres.2020.110011

Gogus, U., & Smith, C. (2010). n-3 Omega fatty acids: A review of current knowledge. *International Journal of Food Science and Technology, 45*(3), 417–436. https://doi.org/10.1111/j.1365-2621.2009.02151.x

Golding, M., J. Wooster, T., Day, L., Xu, M., Lundin, L., Keogh, J., & Clifton, P. (2011). Impact of gastric structuring on the lipolysis of emulsified lipids. *Soft Matter, 7*(7), 3513–3523. https://doi.org/10.1039/C0SM01227K

Gong, X., Hui, X., Wu, G., Morton, J. D., Brennan, M. A., & Brennan, C. S. (2022). In vitro digestion characteristics of cereal protein concentrates as assessed using a pepsin-pancreatin digestion model. *Food Research International, 152*, Article 110715. https://doi.org/10.1016/j.foodres.2021.110715

Hasanvand, E., & Rafe, A. (2018). Characterization of flaxseed gum/rice bran protein complex coacervates. *Food Biophysics, 13*(4), 387–395. https://doi.org/10.1007/s11483-018-9544-5

Hasanvand, E., & Rafe, A. (2019). Development of vanillin/β-cyclodexterin inclusion microcapsules using flax seed gum-rice bran protein complex coacervates. *International Journal of Biological Macromolecules, 131*, 60–66. https://doi.org/10.1016/j.ijbiomac.2019.03.066

Hasanvand, E., Rafe, A., & Emadzadeh, B. (2018). Phase separation behavior of flaxseed gum and rice bran protein complex coacervates. *Food Hydrocolloids, 82*, 412–423. https://doi.org/10.1016/j.foodhyd.2018.04.015

Huang, K., Yuan, Y., & Baojun, X. (2021). A critical review on the microencapsulation of bioactive compounds and their application. *Food Reviews International*, 1–41. https://doi.org/10.1080/87559129.2021.1963978, 0(0).

Hur, S. J., Decker, E. A., & McClements, D. J. (2009). Influence of initial emulsifier type on microstructural changes occurring in emulsified lipids during in vitro digestion. *Food Chemistry, 114*(1), 253–262. https://doi.org/10.1016/j.foodchem.2008.09.069

Hu, Z., Wu, P., Wang, L., Wu, Z., & Dong Chen, X. (2022). Exploring in vitro release and digestion of commercial DHA microcapsules from algae oil and tuna oil with whey protein and casein as wall materials. *Food & Function, 13*(2), 978–989. https://doi.org/10.1039/D1FO02993B

Joyce, P., Gustafsson, H., & Prestidge, C. A. (2018). Enhancing the lipase-mediated bioaccessibility of omega-3 fatty acids by microencapsulation of fish oil droplets within porous silica particles. *Journal of Functional Foods, 47*, 491–502. https://doi.org/10.1016/j.jff.2018.06.015

Kanner, J., & Lapidot, T. (2001). The stomach as a bioreactor: Dietary lipid peroxidation in the gastric fluid and the effects of plant-derived antioxidants. *Free Radical Biology and Medicine, 31*(11), 1388–1395. https://doi.org/10.1016/S0891-5849(01)00718-3

Laemmli, U. K. (1970). Cleavage of structural proteins during the assembly of the head of bacteriophage T4. *Nature, 227*(5259), 680–685. https://doi.org/10.1038/227680a0

Li, R., Lund, P., Nielsen, S. B., & Lund, M. N. (2022). Formation of whey protein aggregates by partial hydrolysis and reduced thermal treatment. *Food Hydrocolloids, 124*, Article 107206. https://doi.org/10.1016/j.foodhyd.2021.107206

Li, Y., & McClements, D. J. (2010). New mathematical model for interpreting pH-stat digestion profiles: Impact of lipid droplet characteristics on in vitro digestibility. *Journal of Agricultural and Food Chemistry, 58*(13), 8085–8092. https://doi.org/10.1021/jf101325m

Li, Y., & McClements, D. J. (2011). Controlling lipid digestion by encapsulation of protein-stabilized lipid droplets within alginate–chitosan complex coacervates. *Food Hydrocolloids, 25*(5), 1025–1033. https://doi.org/10.1016/j.foodhyd.2010.09.024

Lin, Q., Liang, R., Williams, P. A., & Zhong, F. (2018). Factors affecting the bioaccessibility of β-carotene in lipid-based microcapsules: Digestive conditions, the composition, structure and physical state of microcapsules. *Food Hydrocolloids, 77*, 187–203. https://doi.org/10.1016/j.foodhyd.2017.09.034

Lin, W., Zhang, H., Wu, J., Wang, Z., Sun, H., Yuan, J., & Chen, S. (2013). A novel zwitterionic copolymer with a short poly(methyl acrylic acid) block for improving both conjugation and separation efficiency of a protein without losing its bioactivity. *Journal of Materials Chemistry B, 1*(19), 2482–2488. https://doi.org/10.1039/C3TB00474K

Li, Y., Wang, H., Wang, L., Qiu, J., Li, Z., & Wang, L. (2023). Milling of wheat bran: Influence on digestibility, hydrolysis and nutritional properties of bran protein during in vitro digestion. *Food Chemistry, 404*, Article 134559. https://doi.org/10.1016/j.foodchem.2022.134559

Lv, A., Liang, Y., Hu, G., Jin, Y., & Fu, X. (2023). Microwave-assisted extraction and ultrasound-assisted glycation of ovomucoid: Structural and functional properties. *ACS Food Science & Technology, 3*(1), 69–76. https://doi.org/10.1021/acsfoodscitech.2c00282

Mat, D. J. L., Souchon, I., Michon, C., & Le Feunteun, S. (2020). Gastro-intestinal in vitro digestions of protein emulsions monitored by pH-stat: Influence of structural

properties and interplay between proteolysis and lipolysis. *Food Chemistry, 311*, Article 125946. https://doi.org/10.1016/j.foodchem.2019.125946

McClements, D. J., Decker, E. A., Park, Y., & Weiss, J. (2008). Designing food structure to control stability, digestion, release and absorption of lipophilic food components. *Food Biophysics, 3*(2), 219–228. https://doi.org/10.1007/s11483-008-9070-y

Nielsen, P.m., Petersen, D., & Dambmann, C. (2001). Improved method for determining food protein degree of hydrolysis. *Journal of Food Science, 66*(5), 642–646. https://doi.org/10.1111/j.1365-2621.2001.tb04614.x

Ni, Y., Gu, Q., Li, J., & Fan, L. (2021). Modulating in vitro gastrointestinal digestion of nanocellulose-stabilized pickering emulsions by altering cellulose lengths. *Food Hydrocolloids, 118*, Article 106738. https://doi.org/10.1016/j.foodhyd.2021.106738

Niu, C., Luo, H., Shi, P., Huang, H., Wang, Y., Yang, P., & Yao, B. (2016). N-glycosylation improves the pepsin resistance of histidine acid phosphatase phytases by enhancing their stability at acidic pHs and reducing pepsin's accessibility to its cleavage sites. *Applied and Environmental Microbiology, 82*(4), 1004–1014. https://doi.org/10.1128/AEM.02881-15

Nooshkam, M., & Varidi, M. (2020). Maillard conjugate-based delivery systems for the encapsulation, protection, and controlled release of nutraceuticals and food bioactive ingredients: A review. *Food Hydrocolloids, 100*, Article 105389. https://doi.org/10.1016/j.foodhyd.2019.105389

Qiu, L., Zhang, M., Adhikari, B., & Chang, L. (2022). Microencapsulation of rose essential oil in mung bean protein isolate-apricot peel pectin complex coacervates and characterization of microcapsules. *Food Hydrocolloids, 124*, Article 107366. https://doi.org/10.1016/j.foodhyd.2021.107366

Rafe, A., Razavi, S. M. A., & Khan, S. (2012). Rheological and structural properties of β-lactoglobulin and basil seed gum mixture: Effect of heating rate. *Food Research International, 49*(1), 32–38. https://doi.org/10.1016/j.foodres.2012.07.017

Rahmani-Manglano, N. E., Tirado-Delgado, M., García-Moreno, P. J., Guadix, A., & Guadix, E. M. (2022). Influence of emulsifier type and encapsulating agent on the in vitro digestion of fish oil-loaded microcapsules produced by spray-drying. *Food Chemistry, 392*, Article 133257. https://doi.org/10.1016/j.foodchem.2022.133257

Razavi, S., Janfaza, S., Tasnim, N., Gibson, D. L., & Hoorfar, M. (2021). Microencapsulating polymers for probiotics delivery systems: Preparation, characterization, and applications. *Food Hydrocolloids, 120*, Article 106882. https://doi.org/10.1016/j.foodhyd.2021.106882

Singh, H., Ye, A., & Horne, D. (2009). Structuring food emulsions in the gastrointestinal tract to modify lipid digestion. *Progress in Lipid Research, 48*(2), 92–100. https://doi.org/10.1016/j.plipres.2008.12.001

Soleimanifar, M., Jafari, S. M., & Assadpour, E. (2020). Encapsulation of olive leaf phenolics within electrosprayed whey protein nanoparticles; production and characterization. *Food Hydrocolloids, 101*, Article 105572. https://doi.org/10.1016/j.foodhyd.2019.105572

Timilsena, Y. P., Adhikari, R., Barrow, C. J., & Adhikari, B. (2017). Digestion behaviour of chia seed oil encapsulated in chia seed protein-gum complex coacervates. *Food Hydrocolloids, 66*, 71–81. https://doi.org/10.1016/j.foodhyd.2016.12.017

Wang, B., Blanch, E., Barrow, C. J., & Adhikari, B. (2017). Preparation and study of digestion behavior of lactoferrin-sodium alginate complex coacervates. *Journal of Functional Foods, 37*, 97–106. https://doi.org/10.1016/j.jff.2017.07.044

Wang, S., Shi, Y., & Han, L. (2018). Development and evaluation of microencapsulated peony seed oil prepared by spray drying: Oxidative stability and its release behavior during in-vitro digestion. *Journal of Food Engineering, 231*, 1–9. https://doi.org/10.1016/j.jfoodeng.2018.03.007

Xu, D., Yuan, F., Gao, Y., Panya, A., McClements, D. J., & Decker, E. A. (2014). Influence of whey protein–beet pectin conjugate on the properties and digestibility of β-carotene emulsion during in vitro digestion. *Food Chemistry, 156*, 374–379. https://doi.org/10.1016/j.foodchem.2014.02.019

Yang, Y., Cui, S., Gong, J., Miller, S. S., Wang, Q., & Hua, Y. (2015). Stability of citral in oil-in-water emulsions protected by a soy protein–polysaccharide Maillard reaction product. *Food Research International, 69*, 357–363. https://doi.org/10.1016/j.foodres.2015.01.006

Zhang, Z., Holden, G., Wang, B., & Adhikari, B. (2023). Maillard reaction-based conjugation of Spirulina protein with maltodextrin using wet-heating route and characterisation of conjugates. *Food Chemistry, 406*, Article 134931. https://doi.org/10.1016/j.foodchem.2022.134931

Zhang, L., Liao, W., Wei, Y., Tong, Z., Wang, Y., & Gao, Y. (2021a). Fabrication, characterization and in vitro digestion of food-grade β-carotene high loaded microcapsules: A wet-milling and spray drying coupling approach. *LWT, 151*, Article 112176. https://doi.org/10.1016/j.lwt.2021.112176

Zhang, Z., Wang, B., Holden, G., Chen, J., & Adhikari, B. (2023). Improving functional properties of Spirulina protein by covalent conjugation followed by complex coacervation processes. *Future Foods, 7*, Article 100239. https://doi.org/10.1016/j.fufo.2023.100239

Zhang, X., Yue, X., Ma, B., Fu, X., Ren, H., & Ma, M. (2021b). Ultrasonic pretreatment enhanced the glycation of ovotransferrin and improved its antibacterial activity. *Food Chemistry, 346*, Article 128905. https://doi.org/10.1016/j.foodchem.2020.128905